

# THE WILD, ELUSIVE SINGULARITIES OF THE $T$ -FRACTAL SURFACE

CHARLES C. JOHNSON AND ROBERT G. NIEMEYER

ABSTRACT. We show that the set of elusive singularities attached to the  $T$ -fractal surface by its metric completion forms a Cantor set, and are wild singularities in the sense of Bowman and Valdez [BV13]. We compute the Hausdorff dimension of this set of singularities, and show each of these singularities has infinitely-many rotational components.

## 1. INTRODUCTION

In this paper we consider the geometry of an infinite genus, finite area translation surface obtained by unfolding the so-called  $T$ -fractal billiard table, previously described in [LMN16] and [LN13a], and, in particular, study the singularities which are attached to this surface by its metric completion. These singularities come in two types: a countable set of conical singularities of angle  $6\pi$ , which come from various corners of the fractal billiard table, and a set of *elusive singularities* which do not appear in any finite rational polygonal approximation of the  $T$ -fractal.

We rely on the fractality of the  $T$ -fractal billiard table (i.e., the similarity across multiple scales) to determine a flat surface. While successive gluings of scaled copies of what we have termed the *quad- $T$  surface* result in a surface, the metric completion, is not a surface. As we will see, the set of elusive singularities is a Cantor set and the geodesic loops about singularities are decreasing in length. Such a geometry thus complicates any attempt to discuss the geodesic flow on the metric completion.

The paper is organized as follows. In Section 2, we give the necessary background on flat surfaces and polygonal billiards. We discuss the geometric and analytic properties of the singularities of a flat surface and provide examples of wild singularities (as defined in [BV13]). In Section 3, the  $T$ -fractal billiard table and the  $T$ -fractal surface are introduced. As previously indicated, such a surface will be built from the so-called quad- $T$  surface shown in Figure 14, this being the focus of Section 4. We then describe some of the geometric and analytic properties of the metric completion of the  $T$ -fractal surface in Section 5. Finally, in Section 6, we show that an elusive singularity of the metric completion of the  $T$ -fractal surface is a wild singularity and is also a limit point of the set of conical singularities of the  $T$ -fractal surface. We conclude the paper with a brief discussion in Section 7.

---

*Date:* September 24, 2018.

*2010 Mathematics Subject Classification.* Primary: 28A80, 51F99. Secondary: 37E35.

*Key words and phrases.* Fractal billiards, translation surfaces, wild singularities, rational polygonal billiard table, billiard table, conical singularity, self-similarity, fractal,  $T$ -fractal, fractal flat surface, elusive singularities.

## 2. BACKGROUND

In this section we recall some necessary background about translation surfaces and polygonal billiards as well as fix notation.

**2.1. Translation surfaces.** There are many equivalent definitions of a translation surface, but for our purposes what is perhaps the simplest definition will suffice.

**Definition 1.** A *translation surface*  $\mathring{X}$  is a surface equipped with an atlas of charts where all chart changes are accomplished by translations.

We will soon see that every translation surface comes with a natural metric which is typically incomplete. Our notation will be to use  $\mathring{X}$  for the initial surface, and  $X$  for its completion;  $\mathring{X}$  represents a surface which may have some “holes” in it and we use the ring above the letter to indicate this.

One way to construct a translation surface is to consider a collection of polygons in the plane with corners removed, and edges identified in pairs such that each edge of a polygon is glued to a parallel edge of the same length by translation subject to the condition that the inward-pointing normal vectors along these edges point in opposite directions.

**Example 1.** Removing the corners from a regular octagon and identifying opposite edges — edges with the same label in Figure 1 — produces a translation surface homeomorphic to a genus two surface with one point removed.

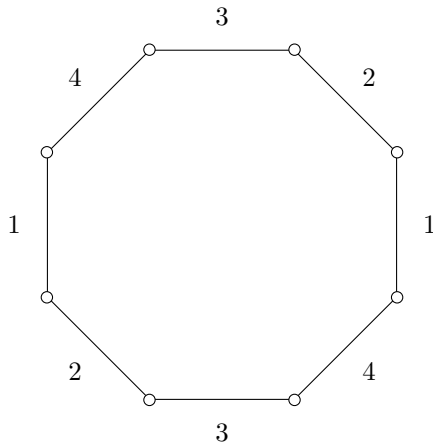


FIGURE 1. Identifying opposite sides of an octagon with vertices removed produces a translation surface.

Alternatively, we may construct a translation surface by integrating a holomorphic 1-form on a Riemann surface. Given a Riemann surface  $X$  and a holomorphic 1-form  $\omega$ , let  $\mathring{X}$  denote the complement of the zeros of  $\omega$ . We may equip  $\mathring{X}$  with a translation atlas by local integration of  $\omega$ . That is, for each point  $P$  in  $\mathring{X}$  we consider a simply-connected neighborhood  $U$  of  $P$  and assign coordinates  $\varphi : U \rightarrow \mathbb{C}$  by declaring  $\varphi(Q) = \int_P^Q \omega$ . Since integration of holomorphic 1-forms in simply-connected domains is independent of path, this gives a well-defined chart.

Furthermore, if two such coordinate charts have a simply-connected intersection, then it is easy to see that a change of coordinates is accomplished by a translation. Supposing  $P_1$  and  $P_2$  are the centers of two charts  $\varphi_1 : U_1 \rightarrow \mathbb{C}$  and  $\varphi_2 : U_2 \rightarrow \mathbb{C}$  and  $Q \in U_1 \cap U_2$ , we see that if

$$\int_{P_1}^Q \omega - \int_{P_2}^Q \omega + \int_{P_1}^{P_2} \omega = 0,$$

then  $\varphi_1(Q) = \varphi_2(Q) - \int_{P_1}^{P_2} \omega$ .

Notice that every open subset of  $\mathbb{C}$  is naturally a translation surface using the identity map as a chart; this corresponds to integrating  $dz$ .

As chart changes are translations, any translation-invariant quantity defined in the plane can be pulled back to  $\mathring{X}$ . In particular, we can define a measure on the surface by pulling back the Lebesgue measure of the plane, and a metric by pulling back the standard Euclidean metric. This metric space will typically not be complete, and we are concerned with how the geometry of the surface extends to those points added by the metric completion, which we will denote by  $X$ .

Translations in the plane preserve direction, and so the translation surface  $\mathring{X}$  comes with a well-defined notion of direction. We may consider geodesic flow on the surface in any given direction, though we may need to delete a subset of the surface for the flow to be defined for all time. There are many interesting questions about the dynamics of this flow, and the authors will study some of those questions for the  $T$ -fractal surface defined below in a forthcoming paper.

The points of  $X \setminus \mathring{X}$  are called *singularities* of the surface and come in several types which we may classify by considering the families of geodesics in  $\mathring{X}$  which approach points of  $X \setminus \mathring{X}$ . The definitions below are equivalent to those of [BV13], but have been modified slightly to better suit the purposes of this paper.

**Definition 2** (Linear approach). A *linear approach* to  $x \in X$  is map  $\gamma : (0, \infty) \rightarrow \mathring{X}$  whose image is a geodesic segment in  $\mathring{X}$  where  $\lim_{t \rightarrow \infty} \gamma(t) = x$ .

**Definition 3** (Directionally equivalent). We will say two linear approaches to  $x$ ,  $\gamma_1$  and  $\gamma_2$ , are *directionally equivalent* if there exist values  $a_1$  and  $a_2$  such that the image of  $(a_1, \infty)$  under  $\gamma_1$  equals the image of  $(a_2, \infty)$  under  $\gamma_2$ . That is, the geodesic segments given by  $\gamma_1$  and  $\gamma_2$  approach the same point of  $X$  from the same direction. We will let  $D[\gamma]$  denote the directional equivalence class of a linear approach  $\gamma$ .

Linear approaches to a given point can be divided into several families where, intuitively, we can rotate one linear approach to  $x$  to another, passing through linear approaches to  $x$ . To make this idea precise we must introduce the idea of a sector of a flat surface.

**Definition 4** (Standard sector). We will define *the standard sector* of radius  $r > 0$  and angle  $\theta > 0$  as the translation surface  $S_{r,\theta}$  obtained by equipping the open strip  $(-\log(r), \infty) \times (-\theta/2, \theta/2)$ , thought of as a subset of the complex plane  $\mathbb{C}$ , with the translation structure obtained by local integration of the 1-form  $\omega = e^{-z} dz$ . We define the sector of angle  $\theta = 0$  and radius  $r > 0$ ,  $S_{r,0}$ , as the ray  $(-\log(r), \infty) \times \{0\}$ . Local integration of  $e^{-z} dz$  gives  $S_{r,0}$  the structure of a translation 1-manifold. We define the sector of infinite angle as the translation surface  $S_{r,\infty}$  obtained by local integration of  $e^{-z} dz$  in the open half-plane  $(-\log(r), \infty) \times (-\infty, \infty) \subseteq \mathbb{C}$ .

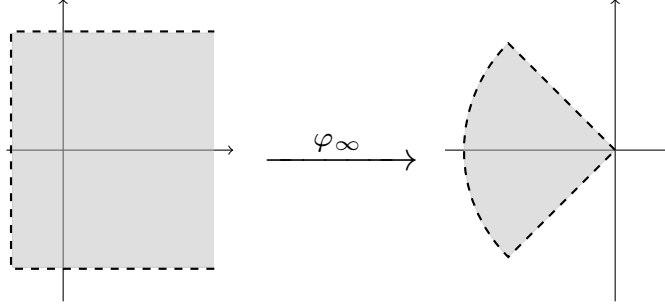


FIGURE 2. The standard sector  $S_{r,\theta}$  equipped with the translation structure coming from  $e^{-z}dz$  is isometric to a sector of the plane for  $\theta < 2\pi$ .

**Example 2.** If  $\theta \in (0, 2\pi)$ , then the standard sector of angle  $\theta$  and any radius  $r > 0$  is equipped with a global chart that makes the standard sector isometric to the following angular sector of a disc of radius  $r$ ,

$$\{(x, y) \in \mathbb{R}^2 \mid 0 < x^2 + y^2 < r^2 \text{ and } \pi - \theta/2 < \arctan(y/x) < \pi + \theta/2\}.$$

In particular, given any point  $P \in S_{r,\theta}$  we have a chart  $\varphi_P : S_{r,\theta} \rightarrow \mathbb{C}$  given by

$$\varphi_P(Q) = \int_P^Q e^{-z} dz = e^{-P} - e^{-Q}.$$

Consider also the chart  $\varphi_\infty : S_{r,\theta} \rightarrow \mathbb{C}$  given by

$$\varphi_\infty(Q) = \lim_{t \rightarrow \infty} \int_{Q+t}^Q e^{-z} dz = -e^{-Q}.$$

Notice this chart is compatible with each of the  $\varphi_P$  charts:

$$\varphi_\infty(Q) = \varphi_P(Q) - e^{-P}.$$

Furthermore, the image of  $\varphi_\infty(S_{r,\theta})$  is precisely the angular sector described above; see Figure 2. Equipping this sector with the usual translation structure given by integrating  $dz$  shows that  $\varphi_\infty$  is in fact an isometry as  $e^{-z}dz = \varphi_\infty^*(dz)$ .

**Definition 5** (Sector). A *sector* of angle  $0 \leq \theta \leq \infty$  and radius  $r > 0$  in a translation surface  $\mathring{X}$  is an isometry  $\psi$  from the standard sector  $S_{r,\theta}$  to an open subset of  $\mathring{X}$ . We will say the sector is *centered* at  $x \in X$  if  $\lim_{z \rightarrow \infty} \psi(z) = x$ . We will sometimes abuse language and refer to the image of  $\psi$  as the sector.

**Definition 6** (Rotationally equivalent). We will say that two linear approaches  $\gamma_1$  and  $\gamma_2$  to  $x \in X$  are *rotationally equivalent* if there exists a sector  $\psi : S_{r,\theta} \rightarrow \mathring{X}$  in  $\mathring{X}$ , centered at  $x$ , such that for some  $y_k \in (-\theta/2, \theta/2)$ ,  $k = 1, 2$ , the map  $t \mapsto \psi(t + iy_k)$  is a linear approach to  $x$  which is directionally equivalent to  $\gamma_k$ .

**Definition 7** (Rotational component). A *rotational component* of  $x \in X$  is a rotational equivalence class of linear approaches to  $x$ , and the supremum of all angles of sectors in  $\mathring{X}$  containing linear approaches in that rotational component is the *length* of the rotational component. If a point has only one rotational component, then we will sometimes refer to the length of that rotational component as the cone angle of the point.

Given two rotationally equivalent linear approaches  $\gamma_1$  and  $\gamma_2$ , let  $\mathcal{S}(\gamma_1, \gamma_2)$  denote the set of all sectors in  $\mathring{X}$  containing linear approaches directionally equivalent to  $\gamma_1$  and  $\gamma_2$ . In such a sector  $\psi : S_{r,\theta} \rightarrow \mathring{X}$  in  $\mathcal{S}(\gamma_1, \gamma_2)$ , there exist  $y_1$  and  $y_2$  such that the maps  $t \mapsto \psi(t + iy_k)$  are linear approaches directionally equivalent to each  $\gamma_k$ . We then define the distance between  $\gamma_1$  and  $\gamma_2$  to be the infimum of the distance between  $y_1$  and  $y_2$ ,  $|y_1 - y_2|$ , taken over all sectors in  $\mathcal{S}(\gamma_1, \gamma_2)$ . This distance function is a metric on the rotational component making it isometric to a subinterval of the real line, or a circle of circumference  $2n\pi$  for some positive integer  $n$ . See [BV13, Remark 1.9] for details.

One simple observation about rotationally equivalent linear approaches which we will use later is the following.

**Lemma 1.** *If  $\gamma_1$  and  $\gamma_2$  are two rotationally equivalent linear approaches to  $x \in X$ , then they have directionally equivalent representatives which do not intersect.*

*Proof.* If this were not the case, then every sector containing  $\gamma_1$  and  $\gamma_2$  would contain linear approaches directionally equivalent to  $\gamma_1$  and  $\gamma_2$ , but which intersect. This contradicts the fact that the sector is isometrically embedded in  $\mathring{X}$  as the rays  $t \mapsto t + iy_k$  mapped to the representatives of  $\gamma_1$  and  $\gamma_2$  do not intersect in the standard sector.  $\square$

We now classify the singularities on a surface based on the number of rotational components and their lengths.

**Definition 8.** Let  $x \in X \setminus \mathring{X}$  be a singularity of the surface.

**Removable singularity:** We say that  $x$  is a *removable singularity* if it has only one rotational component, and that rotational component is isometric to a circle of circumference  $2\pi$ . In this case, a neighborhood of  $x$  is isometric to a disc in the plane.

**(Finite angle) conical singularity:** We say that  $x$  is a *(finite angle) conical singularity* if it has only one rotational component, and that rotational component is isometric to a circle of circumference  $2n\pi$  for some positive integer  $n$ . In this case, a punctured neighborhood of  $x$  is isometric a cyclic  $n$ -cover of the punctured disc.

**Infinite angle conical singularity:** We say that  $x$  is an *infinite angle conical singularity* if it has only one rotational component, and that rotational component is isometric to an infinite length subinterval of the real line. In this case, a punctured neighborhood of  $x$  is isometric to an infinite cover of the punctured disc.

**Wild singularity:** In all other situations we say  $x$  is a *wild singularity*.

We now give examples of surfaces with each type of singularity.

**Example 3.** Consider the unit square with each of its four vertices removed. Identifying the interiors of opposite sides of the square gives a surface  $\mathring{X}$  which is a torus with a single point removed. The metric completion fills in this hole with a removable singularity, and the shaded regions in Figure 3 form a neighborhood of the singularity which glue together to give a disc on the torus.

**Example 4.** Identifying opposite sides of a regular decagon gives a genus two translation surface with two singularities, both of which are conical singularities of angle  $4\pi$ . In Figure 4, the vertices which have sectors of the same shade of grey

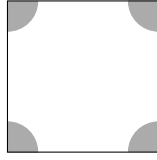


FIGURE 3. The four vertices of the unit square give rise to a removable singularity on the torus.

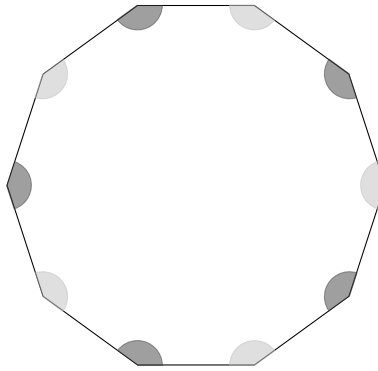


FIGURE 4. The regular decagon surface.

are identified to a single conical singularity of angle  $4\pi$ . The shaded sectors of the conical points in Figure 4 glue together to give a neighborhood of the point which is a double cover of a disc as indicated in Figure 5.

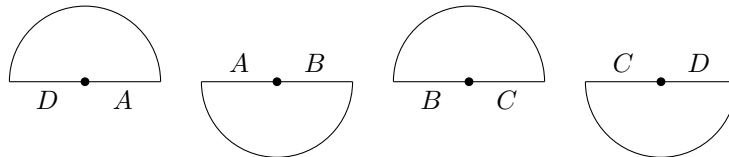


FIGURE 5. Identifying edges with the same label produces a Euclidean cone of angle  $4\pi$ .

**Example 5.** The metric completion of the standard sector  $S_{r,\theta}$ ,  $0 \leq \theta \leq \infty$ , adds to the surface an additional point at infinity with one rotational component which has angle  $\theta$ . If  $\theta = 2\pi$ , the point at infinity is a removable singularity; if  $\theta = 2n\pi$  for some integer  $n > 1$ , then the point at infinity is a conical singularity; if  $\theta = \infty$ , then the point at infinity is an infinite angle conical singularity; in all other cases the point at infinity is a wild singularity.

The boundary points of the subset of the plane giving  $S_{r,\theta}$  are wild singularities. See Figure 6.

**Example 6.** The following *infinite staircase* surface was studied by Hooper, Hubert, and Weiss in [HHW13]. Take a countably infinite collection of rectangles of

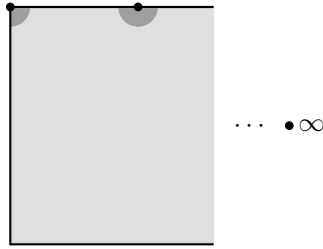


FIGURE 6. The metric completion of the standard sector  $S_{r,\theta}$ . The point at infinity is marked  $\infty$ . Two points, which are technically wild singularities of cone angles  $\pi/2$  and  $\pi$  are indicated.

size  $2 \times 1$ , and stack them so the left-hand half of each rectangle is directly above the right-hand half of the rectangle below it. Identifying opposite sides in pairs produces an infinite genus surface with four infinite angle conical singularities as indicated in Figure 7.

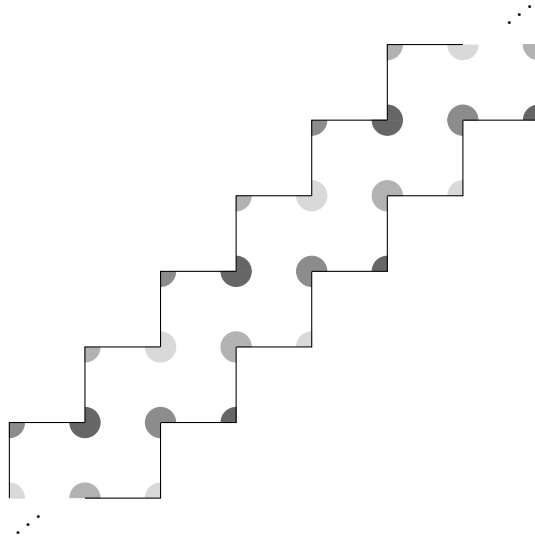


FIGURE 7. The staircase surface has four infinite angle conical singularities.

**Example 7.** The following example is due to Chamanara [Cha04]. Consider taking a unit square and cutting each edge into pieces of length  $1/2, 1/4, 1/8, \dots$  with parallel edges cut in opposite orders, and then identify parallel edges of the same length as indicated in Figure 8. The metric completion of this surface adds a single point corresponding to the corners of the square and the endpoints of the cuts, and this is a wild singularity: no neighborhood of this point can be isometric to a cover of the punctured disc as there are arbitrarily short geodesic loops based at the singularity.

**2.2. Polygonal billiards.** Translation surfaces naturally arise in the study of polygonal billiards because they allow the tools of differential geometry to be used

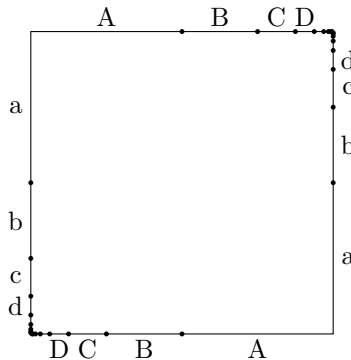


FIGURE 8. The Chamanara surface. Parallel edges of the same length are identified. The first few horizontal and vertical identifications are labeled in this diagram.

to study the dynamics of billiards. More precisely, given a polygonal subset  $P$  of the plane, called a *billiard table*, we may consider the motion of an ideal point-mass, called a *billiard ball*, inside that region. The billiard ball moves in a straight line in the interior of the polygon at unit speed until reaching the boundary of the polygon. Upon reaching the boundary the billiard ball is reflected off the boundary according to the rule that the angle of incidence equals the angle of reflection, and then continues to move in a straight line at unit speed in this new direction. This gives a dynamical system, and we may ask questions about this system concerning the long-term behavior of the billiard ball. To study dynamical questions about the billiard it is convenient to turn the questions about billiard paths into questions about geodesics on a surface, and this is accomplished through a process called *unfolding* and first introduced in [ZK75].

One way to describe the unfolding procedure is as follows. Let  $P$  denote a polygonal billiard table, and to each side  $s$  of  $P$  associate a linear reflection  $r_s$  across the line parallel to  $s$  through the origin in the plane. Let  $G$  denote the group generated by these reflections. If  $P$  is simply connected and all interior angles of  $P$  are rational multiples of  $\pi$ , then  $G$  will be a finite group. For each  $g \in G$ , let  $P_g$  denote the image of  $P$  under  $g$ . We identify the images of a side  $s$  in  $P_g$  and  $P_{g'}$  by translation if  $g' = r_s g$ . This identifies edges of the  $P_g$  polygons in pairs where each edge is identified with a parallel edge of the same length by a translation.

**Example 8.** Let  $P$  be the triangle with interior angles  $\frac{\pi}{2}$ ,  $\frac{\pi}{10}$ , and  $\frac{2\pi}{5}$ , labeling the sides of the triangle  $A$ ,  $B$ , and  $C$  as indicated in Figure 9.

Now consider the group  $G$  generated by linear reflections parallel to the edges  $A$ ,  $B$ , and  $C$ ,

$$\langle r_A, r_B, r_C \mid r_A^2, r_B^2, r_C^2, (r_A r_B)^{20}, (r_B r_A)^{20}, (r_A r_C)^5, (r_C r_A)^5, (r_B r_C)^4, (r_C r_B)^4 \rangle.$$

This group has order twenty, and so gives twenty reflected copies of the triangle which we glue together at their edges to obtain a translation surface. In this example the twenty triangles glue together to give the regular decagon surface of Figure 4.



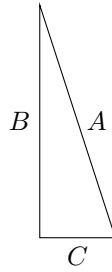


FIGURE 9. The triangle with interior angles  $\frac{\pi}{2}$ ,  $\frac{\pi}{10}$  and  $\frac{2\pi}{5}$  with labeled sides.

3. THE  $T$ -FRACTAL BILLIARD TABLE AND  $T$ -FRACTAL SURFACE

3.1. **The billiard table.** We now describe the construction of a fractal billiard table in the plane which we will unfold to obtain a non-compact translation surface. The region we will consider will be a countable union of polygonal regions in the plane which are built iteratively.

The  $T$ -shaped polygon is the polygon indicated in Figure 10 which we will denote  $T_0$ .

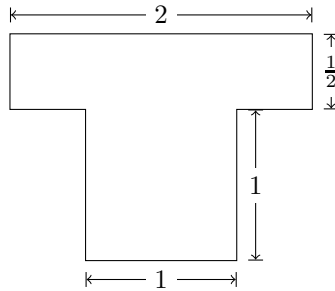


FIGURE 10. The T-shaped polygon,  $T_0$ .

The  $n$ -th level approximation of the  $T$ -fractal, denoted  $T_n$ , is obtained from  $T_{n-1}$  by attaching  $2^n$  copies of  $T_0$ , each scaled by  $2^{-n}$ , to the top left- and right-hand portions of the scaled copies of  $T_0$  sitting at the top of  $T_{n-1}$ . See Figure 11 for the cases of  $T_0$  through  $T_3$ .

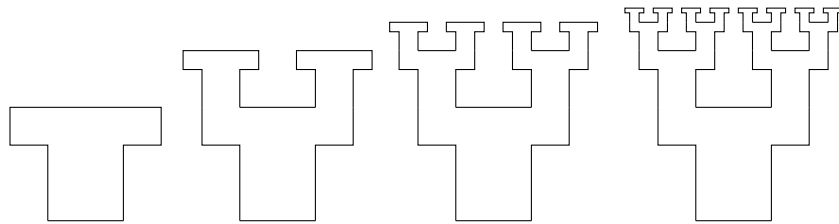


FIGURE 11. The iterative construction of the  $T$ -fractal billiard table.

**Definition 9** (*T*-fractal billiard table). We define the *T*-fractal billiard table, denoted  $T_\infty$ , as the union of all the  $n$ -th level approximations,

$$T_\infty = \bigcup_{n=0}^{\infty} T_n.$$

See Figure 12 for an illustration of  $T_\infty$ .

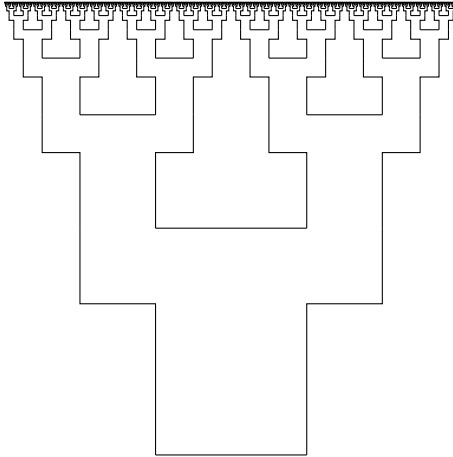


FIGURE 12. The *T*-fractal billiard table,  $T_\infty$ .

**Remark 1.** How we have defined  $T_\infty$  differs from how the second author has defined  $T_\infty$  in previous joint papers, e.g., [LN13a] and [LMN16]. Specifically, in previous papers,  $T_\infty$  was defined to be the closure of  $\bigcup_{n=0}^{\infty} T_n$  and the notation for the billiard table was actually  $\Omega(T_\infty)$ . The change to simpler notation and an alternate description of  $T_\infty$  facilitates our construction of the *T*-fractal surface shown in Figure 13. In previous articles, the set of elusive points of the *T*-fractal billiard was a subset of the *T*-fractal billiard and constituted a connected interval. What we will show is that the set of elusive singularities of the *T*-fractal surface is a totally disconnected set and is only present in the metric completion of the *T*-fractal surface, and the metric completion of the *T*-fractal surface is in fact not a surface.

**3.2. Unfolding  $T_\infty$ .** Though  $T_\infty$  is not strictly a polygonal region, the unfolding procedure may still be applied to obtain a translation surface whose geodesics project to billiard trajectories in  $T_\infty$ . In particular,  $T_\infty$  consists only of horizontal and vertical edges, so the group generated by linear reflections in its sides is the group generated by two orthogonal reflections: the Klein four-group,  $\mathbb{Z}_2 \oplus \mathbb{Z}_2$ .

**Definition 10.** The *T*-fractal surface, denoted  $\mathring{\mathcal{T}}$ , is the surface obtained by unfolding the *T*-fractal billiard table,  $T_\infty$ . This surface is made from four copies of the *T*-fractal billiard table with edge identifications as indicated in Figure 13.

The surface  $\mathring{\mathcal{T}}$  is not a complete metric space, and so we consider its metric completion which we will denote  $\mathcal{T}$ . A first observation about  $\mathcal{T}$  is that it contains infinitely-many cone points of cone angle  $6\pi$  coming from the corners of  $T_0$  (and

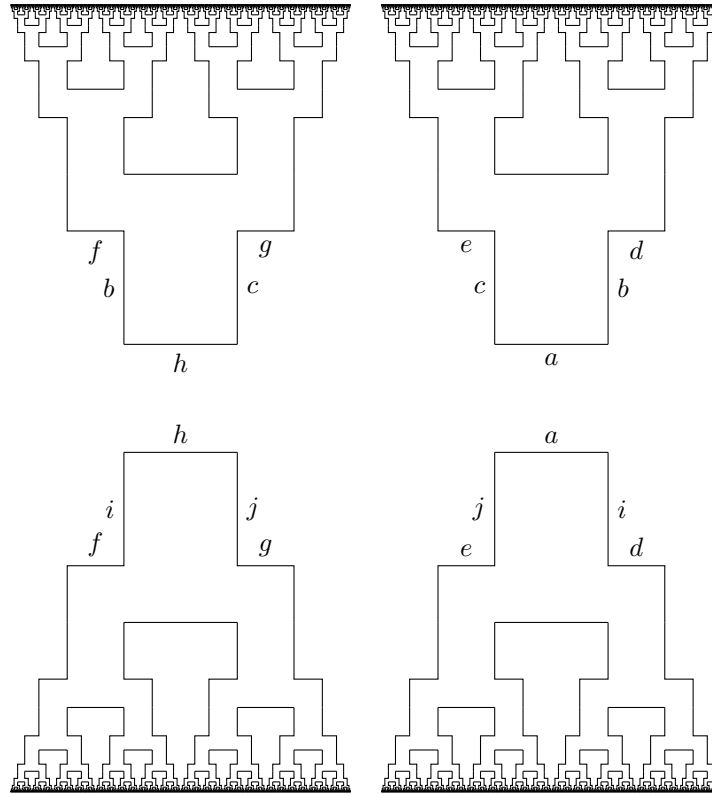


FIGURE 13. The surface  $\hat{\mathcal{T}}$ . Only the first few edges in the copies of the billiard table  $T_\infty$  are labeled to indicate how sides are glued together to form  $\hat{\mathcal{T}}$ .

so each  $T_n$ ) where the  $2 \times 1/2$  rectangle is placed on top of the  $1 \times 1$  square. The singular points in  $\mathcal{T} \setminus \hat{\mathcal{T}}$  which are more interesting, however, are those points which come from the “top” of the  $T$ -fractal. In previous work of Lapidus and Niemeyer, these were called the *elusive points* of the  $T$ -fractal, and so we will refer to these as *elusive singularities* of the  $T$ -fractal surface,  $\hat{\mathcal{T}}$ . (A precise definition of elusive singularities is given below.)

In order to study the elusive singularities of  $\hat{\mathcal{T}}$  we will consider a special class of compact translation surfaces with boundary which are embedded in  $\hat{\mathcal{T}}$  and which we call *quad- $T$  subsurfaces*.

#### 4. THE QUAD- $T$ SUBSURFACES

Just as we imagine the  $T$ -fractal billiard  $T_\infty$  as being built from scaled copies of the original  $T$ -shaped polygon, we may imagine the surface  $\hat{\mathcal{T}}$  as being built from scaled copies of a certain translation surface with boundary indicated in Figure 14. We call the surface  $\mathcal{Q}$  of Figure 14 a *quad- $T$  surface*. The surface  $\hat{\mathcal{T}}$  is obtained by gluing scaled copies of  $\mathcal{Q}$  together at their boundary components. To distinguish the different copies of the quad- $T$  surface in  $\hat{\mathcal{T}}$ , we index the copies by binary strings.

Let  $\mathcal{B} = \{0, 1\}$ , and let  $\mathcal{B}^*$  be the set of all finite binary strings with  $\epsilon$  denoting the empty string. For each string  $s \in \mathcal{B}^*$ , let  $\mathcal{Q}^s$  denote a copy of  $\mathcal{Q}$  scaled by  $2^{-|s|}$  where  $|s|$  is the length of the string  $s$ . Labeling the boundary components of  $\mathcal{Q}$  as indicated in Figure 14, we let  $\gamma_1^s, \dots, \gamma_6^s, \sigma_1^s, \dots, \sigma_6^s$  denote the corresponding boundary components of  $\mathcal{Q}^s$ .

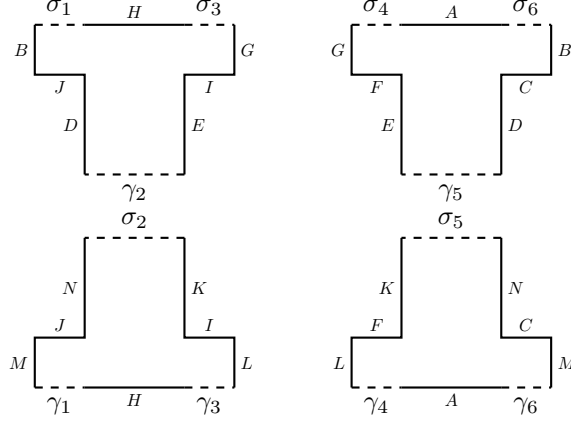


FIGURE 14. The quad-T surface,  $\mathcal{Q}$ . Dashed line segments are boundary components, and solid line segments with the same label are identified by translation.

We may reconstruct the surface  $\mathring{\mathcal{T}}$  by gluing these quad-T subsurfaces together at their boundary components, with each  $\gamma$  component glued to some  $\sigma$  component. Precisely, we identify  $\gamma_2^\epsilon \sim \sigma_2^\epsilon$  and  $\gamma_5^\epsilon \sim \sigma_5^\epsilon$ , and then for each string  $s$  we perform the following identifications:

$$\begin{aligned} \sigma_1^s &\sim \gamma_2^{s1}, & \sigma_6^s &\sim \gamma_5^{s1}, \\ \gamma_1^s &\sim \sigma_2^{s1}, & \gamma_6^s &\sim \sigma_5^{s1}, \\ \sigma_3^s &\sim \gamma_2^{s0}, & \sigma_4^s &\sim \gamma_5^{s0}, \\ \gamma_3^s &\sim \sigma_2^{s0}, & \gamma_4^s &\sim \sigma_5^{s0}. \end{aligned}$$

All identifications are translations between parallel line segments of equal length, and the above identifications give the surface  $\mathring{\mathcal{T}}$ . We may thus think of each  $\mathcal{Q}^s$  as being embedded in  $\mathring{\mathcal{T}}$ ; see Figure 15. When discussing quad-T subsurfaces, we will let  $\mathcal{Q}$  and  $\mathcal{Q}^s$  refer to the metric completions of the surface in Figure 14.

## 5. THE METRIC COMPLETION OF $\mathring{\mathcal{T}}$

In order to understand the points added by the metric completion of  $\mathring{\mathcal{T}}$ , we will show that equivalence classes of Cauchy sequences on  $\mathring{\mathcal{T}}$  which do not converge to a point of  $\mathring{\mathcal{T}}$  may be thought of as increasing sequences of quad-T subsurfaces.

**Definition 11.** We define an *elusive singularity* to be a point of  $\mathcal{T}$  which is not contained in any quad-T subsurface and denote the set of elusive singularities  $\mathcal{E}$ ,

$$\mathcal{E} = \mathcal{T} \setminus \bigcup_{s \in \mathcal{B}^*} \mathcal{Q}^s.$$



one more bit appended to the right). In all other cases the distance is bounded below by a positive constant depending on  $|s|$  and  $|t|$ .

*Proof.* First consider the case that  $s \wedge t = s$ , and so  $t = st'$  for some string  $t' \in \mathcal{B}^*$ . If  $|t'| = 1$ , then  $\mathcal{Q}^s$  and  $\mathcal{Q}^t$  connect at a boundary component, and so  $\text{dist}(\mathcal{Q}^s, \mathcal{Q}^t) = 0$ . If  $|t'| \geq 2$ , suppose  $t' = b_1 b_2 \dots b_n$  are the bits of  $t'$ . A geodesic connecting a point of  $\mathcal{Q}^s$  to  $\mathcal{Q}^t$  would have to pass through the intermediate subsurfaces  $\mathcal{Q}^{sb_1}$ ,  $\mathcal{Q}^{sb_2}$ , ...,  $\mathcal{Q}^{sb_{n-1}}$  and cannot have arbitrarily small length.

Now, if  $|s| = |t| = 1$  with  $s \neq t$  (i.e.,  $s = 0$  and  $t = 1$  or vice versa), then  $\text{dist}(\mathcal{Q}^s, \mathcal{Q}^t) \geq 1$ . This follows from the fact that a geodesic between  $\mathcal{Q}^s$  and  $\mathcal{Q}^t$  must pass into  $\mathcal{Q}^\epsilon$  passing through two distinct boundary components, and the distance between any two boundary components is at least 1. In general, for  $s$  and  $t$  the same string except for the last (right-most) bit, we have that  $\text{dist}(\mathcal{Q}^s, \mathcal{Q}^t) \geq 2^{-|s \wedge t|}$ . If  $s \wedge t = s$  and  $t = st'$ , for some  $t' \in \mathcal{B}^*$  of length  $n$ , this means that a geodesic connecting  $\mathcal{Q}^s$  to  $\mathcal{Q}^t$  has length at least

$$(1) \quad \sum_{i=1}^{n-1} 2^{i-|s|} = 2^{-|s|} \sum_{i=1}^{n-1} 2^{-i} = \frac{1}{2^{|s|}} \cdot \frac{2^{n-1} - 1}{2^{n-1}},$$

since a geodesic must pass through every quad-T subsurface between  $\mathcal{Q}^s$  and  $\mathcal{Q}^t$ . As  $n = |t| - |s|$ , the distance from  $\mathcal{Q}^s$  to  $\mathcal{Q}^t$  when  $s \wedge t = s$  is bounded below:

$$(2) \quad \text{dist}(\mathcal{Q}^s, \mathcal{Q}^t) \geq \frac{2^{|t|-|s|-1} - 1}{2^{|t|-1}}.$$

The general case  $s = (s \wedge t)s'$  and  $t = (s \wedge t)t'$ , for some  $s', t' \in \mathcal{B}^*$ , reduces to the above by noticing that a geodesic from  $\mathcal{Q}^s$  to  $\mathcal{Q}^t$  must pass through  $\mathcal{Q}^{s \wedge t}$ . In this case,

$$(3) \quad \text{dist}(\mathcal{Q}^s, \mathcal{Q}^t) \geq \frac{2^{|t|-|s \wedge t|-1} - 1}{2^{|t|-1}} + \frac{2^{|s|-|s \wedge t|-1} - 1}{2^{|s|-1}} + 2^{-|s \wedge t|}.$$

□

Similarly, there is an upper bound on how close two points contained in a quad-T subsurface may be from one another.

**Lemma 3.** *There exists a real number  $M$  such that for each  $s \in \mathcal{B}^*$  the diameter of a quad-T subsurface  $\mathcal{Q}^s \subseteq \mathring{\mathcal{T}}$  is bounded above by  $M \cdot 2^{-|s|}$ .*

*Proof.* The Euclidean metric on the quad-T surface  $\mathcal{Q}$  gives a continuous function  $d : \mathcal{Q} \times \mathcal{Q} \rightarrow \mathbb{R}$ . Since  $\mathcal{Q}$  is compact, this function attains a finite upper bound  $M$  which is the diameter of  $\mathcal{Q}$ . Each surface  $\mathcal{Q}^s$  is a rescaling of  $\mathcal{Q}$  by  $2^{-|s|} \leq 1$ , and so the diameter of  $\mathcal{Q}^s$  is  $M \cdot 2^{-|s|}$ . □

**Definition 12** (Branch of  $\mathcal{T}$  rooted at  $\mathcal{Q}^s$ ). For each  $s \in \mathcal{B}^*$  we define a *branch of  $\mathcal{T}$  rooted at  $\mathcal{Q}^s$* , denoted  $\mathcal{B}^s$ , to be the union of all quad-T subsurfaces whose indexing string contains  $s$  as a substring,

$$\mathcal{B}^s = \bigcup_{t \in \mathcal{B}^*} \mathcal{Q}^{st}.$$

Notice the set of elusive singularities may be described as  $\mathcal{E} = \mathcal{T} \setminus \mathcal{B}^\epsilon$ .

**Lemma 4.** *The diameter of each branch  $\mathcal{B}^s$  of  $\mathring{\mathcal{T}}$  is bounded above by  $3M \cdot 2^{-|s|}$  where  $M$  is the upper bound from Lemma 3.*

*Proof.* Let  $x, y \in \mathcal{B}^s$  and suppose  $x \in \mathcal{Q}^{st_1}$  and  $y \in \mathcal{Q}^{st_2}$ . As we are trying to obtain an upper bound on  $d(x, y)$ , we may replace  $x$  and  $y$  with other points in  $\mathcal{Q}^{st_1}$  and  $\mathcal{Q}^{st_2}$  that are further away than the originally chosen  $x$  and  $y$  if necessary. In particular, since  $\text{dist}(\mathcal{Q}^{st_1}, \mathcal{Q}^{st_2}) \leq \text{dist}(\mathcal{Q}^{st_1}, \mathcal{Q}^{st_2\tau})$  for any  $\tau \in \mathcal{B}^*$ , we may suppose that  $|t_1| = |t_2|$ .

We get an upper bound on  $d(x, y)$  by finding a geodesic from  $x$  down to a point in  $\mathcal{Q}^s$ , and then from this point back up to  $y$ . The length of this geodesic in each of the intermediate quad-T subsurfaces has length no greater than the diameter of the quad-T. Hence we sum these diameters to obtain the following, supposing  $|t_1| = |t_2| = n$ :

$$\begin{aligned} d(x, y) &\leq \frac{M}{2^{|s|}} + 2 \sum_{k=1}^n \frac{M}{2^{|s|+k}} \\ &= \frac{M}{2^{|s|}} \left( 1 + \sum_{k=0}^{n-1} \frac{1}{2^k} \right) \\ &= \frac{M}{2^{|s|}} (1 + 2(1 - 2^{-n})). \end{aligned}$$

This diameter increases as  $n$  increases (i.e., as the points move further up the branch  $\mathcal{B}^s$ ), and taking the limit as  $n \rightarrow \infty$  gives the inequality.  $\square$

To describe points of  $\mathcal{E}$  we need to consider Cauchy sequences of points of  $\mathring{\mathcal{T}}$  which do not converge in  $\mathcal{B}^c$ . We will show that equivalence classes of these Cauchy sequences, and hence points of  $\mathcal{E}$ , can be thought of as infinite binary strings where the bits of the string tell us how to climb from the branch  $\mathcal{B}^c$  up to an elusive point. The proof of this fact is broken down into several steps presented as lemmas below.

To ease the language of some of the arguments to come, we introduce a map  $\sigma : \mathring{\mathcal{T}} \rightarrow \mathcal{B}^*$  by setting  $\sigma(x) = s$  if  $x \in \mathcal{Q}^s$ . We adopt the convention that if  $x$  is on a boundary component of a quad-T, and so belongs to two different quad-T's,  $\sigma(x)$  gives the shorter label. For example, if  $x \in \mathcal{Q}^{101} \cap \mathcal{Q}^{1011}$ , then  $\sigma(x) = 101$ .

**Lemma 5.** *If  $(x_n)_{n \in \mathbb{N}}$  is a Cauchy sequence in  $\mathring{\mathcal{T}}$  which does not converge to a point of  $\mathring{\mathcal{T}}$ , then  $|\sigma(x_n)| \rightarrow \infty$  as  $n \rightarrow \infty$ . Passing to a subsequence, we may assume that  $|\sigma(x_n)|$  is strictly increasing.*

*Proof.* Let  $\mathcal{T}_n$  denote the metric completion of the unfolding of  $T_n$ , the  $n$ -th level approximation of the  $T$ -fractal described in Figure 11, and let  $\mathcal{P}_n$  denote the closure of the union of all quad-T surfaces  $\mathcal{Q}^s$  in  $\mathring{\mathcal{T}}$  with  $|s| \leq n$ :

$$\mathcal{P}_n = \overline{\bigcup_{|s| \leq n} \mathcal{Q}^s}.$$

Note that  $\mathcal{P}_n$  may be thought of as a closed subset of any  $\mathcal{T}_m$  with  $m > n$ , as well as a closed subset of  $\mathring{\mathcal{T}}$ , and that these embedded subsets are homeomorphic. As  $\mathcal{P}_n$  is a closed subset of the compact surface  $\mathcal{T}_m$  for  $m > n$ , it is compact and hence a complete metric space.

If  $(x_n)_{n \in \mathbb{N}}$  is a Cauchy sequence in  $\mathring{\mathcal{T}}$  which does not converge, it can not be contained in any  $\mathcal{P}_n$  and so  $\sup |\sigma(x_n)| = \infty$ . As the sequence  $(x_n)_{n \in \mathbb{N}}$  is Cauchy, we must have  $|\sigma(x_n)| \rightarrow \infty$ .  $\square$

**Lemma 6.** *If  $(x_n)_{n \in \mathbb{N}}$  is a Cauchy sequence in  $\overset{\circ}{\mathcal{T}}$  which does not converge to a point of  $\mathcal{B}^\epsilon$ , then there exists an equivalent Cauchy sequence  $(y_n)_{n \in \mathbb{N}_0}$  of  $\overset{\circ}{\mathcal{T}}$  where for each  $n$ ,  $|\sigma(y_n)| = n$  and  $\sigma(y_n) \wedge \sigma(y_{n+1}) = \sigma(y_n)$ .*

*Proof.* By Lemma 5 we may assume that  $(|\sigma(x_n)|)_{n \in \mathbb{N}}$  is a strictly increasing sequence. Let  $j \in \mathbb{N}_0$ . Since  $(x_n)_{n \in \mathbb{N}}$  is a Cauchy sequence, there exists  $N_j \in \mathbb{N}$  such that for all  $m, n > N_j$  we have  $d(x_m, x_n) < 2^{-j}$ . We must then have that for each  $m, n > N_j$ ,

$$|\sigma(x_m) \wedge \sigma(x_n)| > j$$

and so the first  $j$  characters of  $\sigma(x_m)$  and  $\sigma(x_n)$  must agree. Now for each  $j$  let  $\sigma_j$  be a string of  $j$  bits agreeing with  $\sigma(x_m) \wedge \sigma(x_n)$  for  $m, n > N_j$ . Now choose  $y_j$  to be any point in  $\mathcal{Q}^{\sigma_j}$ . By construction,  $\sigma(y_{j+1})$  is  $\sigma(y_j)$  with a single bit appended. By Lemma 4, for  $n > N_j$ ,  $d(x_n, y_j)$  is at most  $3 \cdot 2^{-|\sigma_j|}$ . Hence the distance between points of the  $(x_n)_{n \in \mathbb{N}}$  sequence and the  $(y_j)_{j \in \mathbb{N}}$  sequence goes to zero and the two sequences determine the same point in the metric completion  $\mathcal{T}$ .  $\square$

**Proposition 7.** *The points of  $\mathcal{E} = \mathcal{T} \setminus \mathcal{B}^\epsilon$  are in one-to-one correspondence with the set of all infinite binary strings.*

*Proof.* By Lemma 6, each point of  $\mathcal{E}$  can be described as the limit of a Cauchy sequence  $(y_j)_{j \in \mathbb{N}}$  where  $\sigma(y_0) = \epsilon$  and  $\sigma(y_{j+1})$  is obtained by appending a single bit to  $\sigma(y_j)$ . That is, the bits of  $\sigma(y_j)$  give an infinite binary string. It remains to show that each point of  $\mathcal{T} \setminus \mathcal{B}^\epsilon$  determines a unique infinite binary string, and each infinite binary string gives a unique point.

Suppose  $x, y \in \mathcal{E}$  and suppose that  $(x_n)_{n \in \mathbb{N}_0}$  and  $(y_n)_{n \in \mathbb{N}_0}$  are Cauchy sequences converging to  $x$  and  $y$ , respectively, where for each  $n$ ,  $|\sigma(x_n)| = n$ ,  $\sigma(x_n) \wedge \sigma(x_{n+1}) = \sigma(x_n)$ , and likewise for the  $\sigma(y_n)$ .

If  $x \neq y$ , then  $\sigma(x_n)$  and  $\sigma(y_n)$  must be equal for each  $n$ : if not, say  $\sigma(x_{n_0}) \neq \sigma(y_{n_0})$ , then by Lemma 2 we must have that  $d(x_n, y_n)$  is bounded below for each  $n > n_0$ . This means that the sequences  $(x_n)_{n \in \mathbb{N}_0}$  and  $(y_n)_{n \in \mathbb{N}_0}$  determine different points of  $\mathcal{E}$ .

If  $\sigma(x_n) = \sigma(y_n)$  for all  $n$ , then  $x_n$  and  $y_n$  are always in the same quad-T subsurface,  $\mathcal{Q}^{\sigma(x_n)} = \mathcal{Q}^{\sigma(y_n)}$ . By Lemma 3,  $d(x_n, y_n) \leq M \cdot 2^{-n}$ , and so  $x = y$ .  $\square$

There are two natural metrics on  $\mathcal{E}$  we may consider. Perhaps the most natural metric for  $\mathcal{E}$  is the metric of  $\mathcal{T}$  restricted to  $\mathcal{E}$ . By Proposition 7 we may also identify each elusive singularity with an infinite binary string, and under this identification it is natural to consider the 2-adic metric on  $\mathcal{E}$ , which we denote  $d_2$ .

**Definition 13.** Given an elusive singularity  $x \in \mathcal{E}$ , let  $\alpha(x)$  denote the corresponding infinite binary string, which we call the *address* of  $x$ . We define the *2-adic metric* on  $\mathcal{E}$  to be the 2-adic metric on the set of binary strings,

$$d_2(x, y) = 2^{-|\alpha(x) \wedge \alpha(y)|}.$$

**Theorem 8.** *The set of elusive singularities  $\mathcal{E}$ , using either the metric  $d$  from  $\mathcal{T}$  or the 2-adic metric  $d_2$ , is a Cantor set of Hausdorff dimension 1.*

*Proof.* Given  $x, y \in \mathcal{E}$ , Lemma 2 and Lemma 4 establish the following inequalities:

$$d_2(x, y) = 2^{-|\alpha(x) \wedge \alpha(y)|} \leq d(x, y) \leq 3M \cdot 2^{-|\alpha(x) \wedge \alpha(y)|} = 3M \cdot d_2(x, y).$$

Thus  $d$  and  $d_2$  define equivalent metrics on  $\mathcal{E}$ . The identity map between these two metric spaces,  $(\mathcal{E}, d)$  and  $(\mathcal{E}, d_2)$ , is thus a bi-Lipschitz map and so preserves



Hausdorff dimension. By Proposition 7,  $(\mathcal{E}, d_2)$  is isometric to the set of 2-adic integers which is known to have Hausdorff dimension 1. In particular,  $(\mathcal{E}, d_2)$  can be thought of as the disjoint union of two copies of itself scaled by  $1/2$ : that is,  $(\mathcal{E}, d_2)$  is the attractor set of an iterated function system defined on itself. In terms of binary strings, the iterated function system is given by two maps,  $\varphi_0$  and  $\varphi_1$ , which append a 0 or a 1, respectively, to the left-hand end of the string:

$$\varphi_0(\sigma) = 0\sigma \quad \text{and} \quad \varphi_1(\sigma) = 1\sigma.$$

The images of  $\varphi_0$  and  $\varphi_1$  are disjoint. Since the collection of 2-adic integers is a compact set (with respect to the 2-adic norm), one can show that the  $s$ -dimensional Hausdorff measure of  $\mathcal{E}$  is finite and nonzero. In the  $d_2$  metric,  $\varphi_0$  and  $\varphi_1$  are similitudes which scale by a factor of  $1/2$ . Therefore,

$$\begin{aligned} (4) \quad H^s(\mathcal{E}) &= H^s(\varphi_0(\mathcal{E})) + H^s(\varphi_1(\mathcal{E})) \\ (5) \quad &= \frac{1}{2^s} H^s(\mathcal{E}) + \frac{1}{2^s} H^s(\mathcal{E}). \end{aligned}$$

The unique solution to this equation is  $s = 1$ . Therefore, the Hausdorff dimension of  $\mathcal{E}$  equipped with either metric is 1.  $\square$

**Theorem 9.** *The metric completion  $\mathcal{T}$  of the surface  $\mathring{\mathcal{T}}$  is not a surface.*

*Proof.* If  $\mathcal{T}$  were a surface, then every point would be contained in some chart domain homeomorphic to an open subset of the plane. In particular, for every point there would exist some  $\epsilon > 0$  so that the  $\epsilon$ -ball centered at that point would be homeomorphic to a disc. We show this is not the case for elusive points by noting that every  $\epsilon$ -ball around an elusive point contains a branch of the  $T$ -fractal: for each elusive singularity  $x \in \mathcal{E}$  and each  $\epsilon > 0$ , there exists a binary string  $s \in \mathcal{B}^*$  such that  $\mathcal{B}^s \subseteq B_\epsilon(x)$ . We now note that  $B_\epsilon(x)$  has a non-trivial first homology group: consider a vertical, geodesic loop  $\gamma$  which passes through two quad- $T$  subsurfaces in  $\mathcal{B}^s$  as shown in Figure 16. The space  $B_\epsilon(x) \setminus \gamma$  remains path-connected, implying  $\gamma$  is homologically non-trivial. Hence for every  $\epsilon > 0$ ,  $H_1(B_\epsilon(x)) \neq 0$ . Consequently  $B_\epsilon(x)$  is not homeomorphic to a disc, so  $\mathcal{T}$  is not a surface.  $\square$

## 6. ELUSIVE SINGULARITIES ARE WILD SINGULARITIES

In this section we show that each elusive singularity of the  $T$ -fractal is a wild singularity.

Recall from Definition 13 that  $\alpha(x)$  is the address of the elusive singularity  $x$ .

**Lemma 10.** *Every elusive singularity  $x$  is a limit point of the set of conical singularities of  $\mathring{\mathcal{T}}$ .*

*Proof.* Suppose that  $x$  is an elusive singularity with address  $\alpha(x) = (\alpha_n)_{n \in \mathbb{N}}$  and let  $\epsilon > 0$  be given. Choose  $k > 0$  such that  $3M \cdot 2^{-k} < \epsilon$ , with  $M$  the number given in Lemma 3. Let  $s$  be the string  $s = \alpha_1 \alpha_2 \cdots \alpha_k$ . The quad- $T$  subsurfaces of the branch  $\mathcal{B}^s$  of the  $T$ -fractal flat surface are then within  $\epsilon$ -distance of  $x$ , and hence so are the conical singularities of those subsurfaces.  $\square$

**Theorem 11.** *Every elusive singularity of the  $T$ -fractal surface is a wild singularity.*

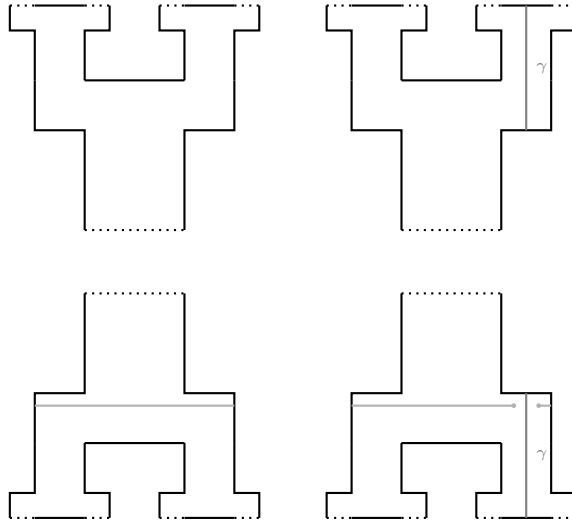


FIGURE 16. A homologically non-trivial curve which passes through two quad-T subsurfaces inside any  $\epsilon$ -ball around an elusive point. The grey, horizontal curve shows that the space remains path-connected even when  $\gamma$  is removed. Only the portions of the quad-T subsurface intersected by the curve are shown.

*Proof.* We simply need to show that each elusive singularity can not be a conical singularity of either finite or infinite angle.

Suppose  $x \in \mathcal{E}$  had a rotational component isometric to a circle. It would then be possible to embed a punctured disc in  $\dot{\mathcal{T}}$  centered at  $x$ . However, this is impossible by Lemma 10 as any neighborhood around an elusive singularity must contain conical singularities. Thus no rotational component of  $x$  is isometric to a circle, and so  $x$  can not be a finite angle conical singularity.

Similarly, if an elusive singularity were an infinite angle conical singularity, then a punctured neighborhood of the point in  $\dot{\mathcal{T}}$  would be an infinite cover of the disc. However, by Lemma 10 this can not be the case since any neighborhood of an elusive singularity contains infinitely-many conical singularities.  $\square$

In [BV13], Bowman and Valdez made the explicit assumption that the singularity set of a translation surface is discrete to rule out certain pathological examples. The Cantor set of singularities on the  $T$ -fractal surface is of course not discrete, and so it is conceivable that some typical notions associated with wild singularities, such as linear approaches and rotational components, are not well-defined or at least not interesting for the  $T$ -fractal surface.

**Lemma 12.** *Every elusive singularity has infinitely-many rotational components.*

*Proof.* To prove this we will consider the action of a particular symmetry of the surface  $\dot{\mathcal{T}}$  on linear approaches to elusive singularities. Notice that each quad-T subsurface has four horizontal cylinders as shown in Figure 17. Two of these cylinders have dimensions  $4 \times 2$ , and so have modulus 2; and the other two cylinders have dimensions  $8 \times 1$  with modulus 8. Thus there exists an affine diffeomorphism

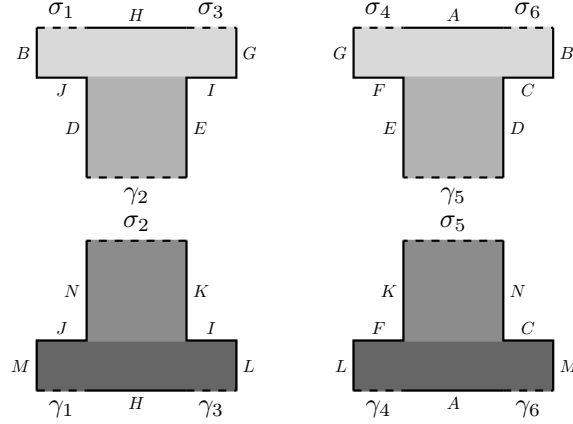


FIGURE 17. Each quad-T subsurface is built from four horizontal cylinders.

with derivative

$$D = \begin{pmatrix} 1 & 8 \\ 0 & 1 \end{pmatrix}$$

acts by twisting these cylinders in such a way that the horizontal foliation in each cylinder is preserved, but the boundaries of the cylinders are fixed pointwise. Since this is true for each quad-T subsurface, there exists some well-defined affine diffeomorphism  $\varphi : \tilde{\mathcal{T}} \rightarrow \tilde{\mathcal{T}}$  with derivative  $D$  acting in the described way on each  $Q^s$ .

Let  $\gamma$  be any linear approach to an elusive singularity. Since  $\varphi$  fixes the boundary components of each horizontal cylinder in each quad-T subsurface,  $\varphi(\gamma)$  is another linear approach to the same elusive singularity. However, because  $\varphi$  twists each cylinder (the  $4 \times 2$  cylinders are twisted four times, and the  $8 \times 1$  cylinders are twisted once),  $\gamma$  and  $\varphi(\gamma)$  intersect in each quad-T containing  $\gamma$  (and hence  $\varphi(\gamma)$ ), as indicated in Figure 18. By Lemma 1, this means that  $\gamma$  and  $\varphi(\gamma)$  can not be rotationally equivalent. Repeating this process by iterating  $\varphi$  generates a sequence of linear approaches to the elusive singularity —  $\gamma, \varphi(\gamma), \varphi^2(\gamma), \dots$  — each of which is in a different rotational component than the other linear approaches in the sequence. Hence, the elusive singularity has infinitely-many rotational components.  $\square$

We gain a finer understanding of the rotational components of an elusive singularity by considering *cutting sequences* of geodesics as they pass the boundaries of the quad-T subsurfaces.

**Definition 14.** Given a geodesic  $\gamma$  of  $\tilde{\mathcal{T}}$ , the *cutting sequence* of  $\gamma$  is the set of labels of quad-T subsurfaces that  $\gamma$  intersects listed in the order in which  $\gamma$  intersects them.

To relate rotational components of elusive singularities to cutting sequences, it will be helpful to define an equivalence relation on cutting sequences.

**Definition 15.** We say that two sequences,  $\omega^1 = (\omega_n^1)_{n \in \mathbb{N}}$  and  $\omega^2 = (\omega_n^2)_{n \in \mathbb{N}}$ , are *eventually equal* if there exist integers  $M$  and  $N$  such that for every  $n > 0$ ,  $\omega_{M+n}^1 = \omega_{N+n}^2$ .

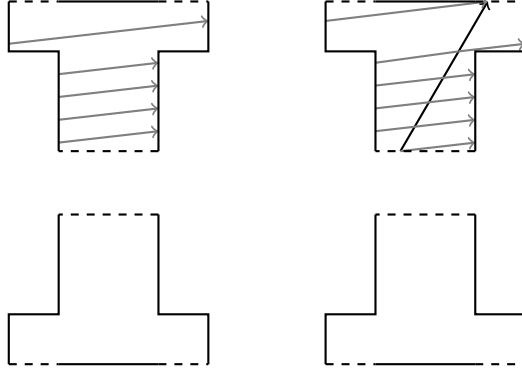


FIGURE 18. Given a geodesic  $\gamma$  (the dark curve in this figure) we construct a new linear approach  $\varphi(\gamma)$  (the lighter curve), which must pass through the same sequence of quad-T's since  $\varphi$  preserves the boundary each quad-T. If  $\gamma$  is a linear approach to an elusive singularity, then  $\varphi(\gamma)$  is another linear approach.

That is, two sequences are eventually equal if they become equal after deleting some finite number of characters, and possibly different numbers of characters from each sequence.

**Example 9.** The sequences

$$\omega^1 = (0, 1, 0, 1, 1, 0, 1, 0, 1, 0, 1, \dots) \text{ and } \omega^2 = (1, 1, 1, 0, 1, 0, 1, 0, 1, \dots),$$

where in both cases the sequence continues to alternate between 0 and 1, are eventually equal:  $\omega_{5+n}^1 = \omega_{3+n}^2$  for all  $n > 0$ .

A first observation about the relationship between cutting sequences and rotational components of elusive singularities is the following.

**Lemma 13.** *If  $\gamma_1$  and  $\gamma_2$  are two rotationally equivalent linear approaches to an elusive singularity, then their cutting sequences are eventually equal.*

*Proof.* If  $\gamma_1$  and  $\gamma_2$  are rotationally equivalent, then there exists a sector containing both linear approaches which is isometrically embedded in  $\hat{\mathcal{T}}$ . Since this sector is embedded in  $\hat{\mathcal{T}}$ , its image in  $\mathcal{T}$  contains no cone points. Thus any boundary component of a quad-T subsurface which intersects the sector must cut all the way across the sector as each boundary component is a loop containing a single cone point. Hence  $\gamma_1$  and  $\gamma_2$  must pass through the same sequences of boundary components of quad-T subsurfaces. See Figure 19 for an illustration.  $\square$

We use these simple observations about cutting sequences in the proof of the following theorem.

**Theorem 14.** *Each rotational component of an elusive singularity has length zero.*

*Proof.* If this were not the case, then there would exist some sector  $\psi : S_{r,\theta} \rightarrow \hat{X}$  with  $\theta > 0$  centered at an elusive singularity  $x$ . Suppose that  $\gamma_1$  and  $\gamma_2$  are two geodesic representatives of linear approaches to  $x$  contained in this sector with respective slopes  $m_1$  and  $m_2$ . We may suppose without loss of generality that  $0 < m_1 < m_2 < \infty$  and the geodesics  $\gamma_1$  and  $\gamma_2$  are parameterized so that the

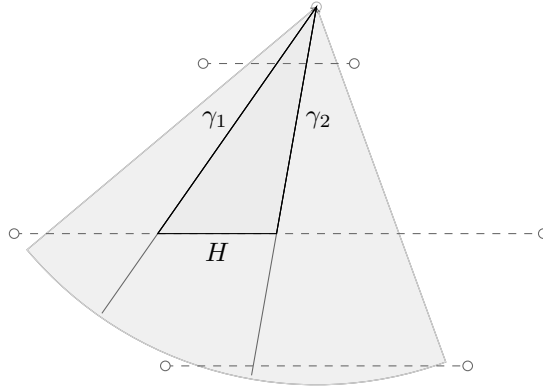


FIGURE 19. An illustration of the quad-T subsurface boundary components cutting across a sector containing two rotationally equivalent linear approaches to an elusive singularity. The dashed lines represent boundary components of quad-T subsurfaces, and the empty circles represent the cone point on the boundary components.

motion along the geodesics,  $t \mapsto \gamma_k(t)$ , moves towards the elusive singularity  $x$  in the North-East direction on the surface.

Suppose that  $\partial Q_0$  is the boundary of some quad-T intersecting with  $\gamma_1$  and  $\gamma_2$  such that the cutting sequences of  $\gamma_1$  and  $\gamma_2$  are equal after passing through  $\partial Q_0$ , and the entries in this cutting sequence are always longer than the label of  $Q_0$  after passing through  $\partial Q_0$ . Let  $H$  denote the horizontal geodesic contained in  $\partial Q_0$  connecting  $\gamma_1$  to  $\gamma_2$ .

From each point  $x \in H$  there exists some slope between  $m_1$  and  $m_2$  such that the geodesic ray fired from  $x$  in the North-East direction, with the appropriately chosen slope, stays inside the triangle with sides  $\gamma_1$ ,  $\gamma_2$ , and  $H$ . Thus there is an isometrically embedded triangle of linear approaches to the wild singularity.

As this triangle is isometrically embedded, we can think of the interior of the triangle as the interior of a triangle in the Euclidean plane. In such a triangle the horizontal distance between the two boundaries meeting at a vertex decreases linearly. That is, the horizontal distance between a point of  $\gamma_1$  and a point of  $\gamma_2$  which are the same vertical distance from the elusive singularity, decreases linearly. However, as a geodesic inside this triangle flows towards the singularity, it must pass through the boundary components of infinitely-many quad-T subsurfaces. Since the quad-T subsurfaces are scaled by factors of  $1/2$ , the lengths of these boundary components decreases exponentially. This means that eventually an endpoint of one of these boundary components must intersect the interior of the triangle bounded by  $\gamma_1$  and  $\gamma_2$ . The endpoints of the boundary components are cone points, however, and our triangle is embedded in  $\mathring{T}$  – the punctured surface without cone points. This contradiction shows that no such triangle can be isometrically embedded into the surface with a vertex at an elusive singularity, and so there can not be any

non-trivial sector (of positive length) containing two such geodesics. Hence each rotational component has zero length.  $\square$

## 7. FINAL REMARKS

There are many questions about the  $T$ -fractal surface that are still unanswered. In particular, classifying the cutting sequences of geodesics on the surface (both infinite-length geodesics and linear approaches to elusive singularities), and determining precisely which directions admit linear approaches to elusive singularities, are two problems the authors believe would be interesting for future research. Perhaps the most obvious questions, however, are concerned with the dynamics of flows on the surface. In a forthcoming paper the authors study these dynamical questions by considering an infinite interval exchange transformation which is the first-return map of the flow to a collection of particular geodesic intervals on the surface.

## REFERENCES

- [BV13] Joshua P. Bowman and Ferrán Valdez, *Wild singularities of flat surfaces*, Israel J. Math. **197** (2013), no. 1, 69–97. MR 3096607
- [Cha04] R. Chamanara, *Affine automorphism groups of surfaces of infinite type*, In the tradition of Ahlfors and Bers, III, Contemp. Math., vol. 355, Amer. Math. Soc., Providence, RI, 2004, pp. 123–145. MR 2145060
- [HHW13] W. Patrick Hooper, Pascal Hubert, and Barak Weiss, *Dynamics on the infinite staircase*, Discrete Contin. Dyn. Syst. **33** (2013), no. 9, 4341–4347. MR 3038066
- [LMN16] Michel L. Lapidus, Robyn L. Miller, and Robert G. Niemeyer, *Nontrivial paths and periodic orbits of the  $t$ -fractal billiard table*, Nonlinearity **29** (2016), no. 7, 2145.
- [LN13a] Michel L. Lapidus, Robert G. Niemeyer, *The current state of fractal billiards*, Fractal Geometry and Dynamical Systems in Pure and Applied Mathematics II: Fractals in Applied Mathematics (Providence, RI) (D. Carfi, M. L. Lapidus, M. van Frankenhuijsen, and E. P. J. Pearse, eds.), vol. 601, Amer. Math. Soc., 2013, pp. 251–288.
- [ZK75] A. N. Zemljakov and A. B. Katok, *Topological transitivity of billiards in polygons*, Mat. Zametki **18** (1975), no. 2, 291–300. MR 0399423 (53 #3267)